Developing an Atomic-Level Understanding to Enhance CO 2 Mineral Sequestration Reaction Processes via Materials and Reaction Engineering

CONFERENCE PAPER · JANUARY 2002

READS
7

5 AUTHORS, INCLUDING:

A. Chizmeshya
Arizona State University
160 PUBLICATIONS **2,375** CITATIONS
SEE PROFILE

Hamdallah Bearat
An-Najah National University
45 PUBLICATIONS **600** CITATIONS
SEE PROFILE

Renu Sharma
mata sundri college, University of Delhi
82 PUBLICATIONS **1,779** CITATIONS
SEE PROFILE

Ray W. Carpenter
Arizona State University
158 PUBLICATIONS **1,683** CITATIONS
SEE PROFILE

Developing an Atomic-Level Understanding to Enhance CO_2 Mineral Sequestration Reaction Processes via Materials and Reaction Engineering

Michael J. McKelvy*#, Andrew V.G. Chizmeshya*, Hamdallah Bearat,# Renu Sharma*#, and R.W. Carpenter*#

* *Center for Solid State Science, Arizona State University, Tempe, Arizona 85287 USA*
# *Science and Engineering of Materials PhD Program, Arizona State University, Tempe, Arizona 85287 USA*

ABSTRACT

Over the last decade, discussion has evolved from whether exponentially increasing anthropogenic CO_2 emissions will adversely affect the global environment, to the timing and magnitude of their impact. A variety of sequestration technologies are being explored to mitigate CO_2 emissions. These technologies must be both environmentally benign and economically viable. Mineral carbonation is an attractive candidate technology as it disposes of CO_2 as geologically stable, environmentally benign mineral carbonates, clearly satisfying the first criteria. The primary challenge for mineral carbonation is cost-competitive process development. Mg-rich lamellar hydroxides offer exciting potential as widely available, low-cost feedstock materials (e.g., serpentines). Furthermore, dehydroxylation offers the intriguing potential to disrupt these materials down to the atomic level, substantially enhancing their carbonation reactivity, a key component in reducing process cost. Over the past year and a half, we have been studying dehydroxylation/carbonation reaction processes for the prototype Mg-rich lamellar-hydroxide: $Mg(OH)_2$. The primary goal is to develop the fundamental mechanistic understanding needed to enhance carbonation reactivity. Recently, we discovered $Mg(OH)_2$ dehydroxylation is best described as a lamellar nucleation and growth process, which can access a range of new, potentially high-surface-area, lamellar oxyhydroxide intermediate materials, $Mg_{x+y}O_x(OH)_{2y}$. These materials provide access to a broad range of new carbonation reaction pathways via dehydroxylation/rehydroxylation, which can dramatically increase carbonation reactivity. Similar mechanisms may be more broadly applicable to Mg/Ca-rich lamellar-hydroxide-based mineral (e.g., serpentine) carbonation processes, offering substantial potential for reducing CO_2 mineral sequestration process costs. This effort is a part of the Mineral Carbonation Study Program managed by DOE, which also includes participants from the Albany Research Center, Los Alamos National Laboratory, the National Energy Technology Laboratory, and Science Applications International Corporation.

INTRODUCTION

Over the last few centuries energy technology has evolved to meet the needs of a growing global economy. A broad range of energy resources has been developed providing the energy infrastructure of today. Fossil fuels have developed a dominant role due to their low cost, wide availability and high energy content.[1,2] 85% of the world's energy needs today are satisfied by fossil fuels, with coal playing the major role. Known coal reserves can easily supply the world's energy needs for centuries to come, as the world economy expands, and energy needs continue their exponential increase.[3-5] However, the development of the global energy infrastructure has been predicated on the critical assumption that anthropogenic CO_2 emissions can continue to increase without adverse environmental consequences. During the 1990's, this assumption came under critical review, with discussion evolving from whether

exponentially increasing anthropogenic CO_2 emissions will have an adverse environmental impact, to the timing and magnitude of their impact.[2] Policies outlined at the 1997 Kyoto Conference aim to severely restrict global carbon dioxide emissions.[6] This is of particular concern to the coal industry as fossil fuel energy production is the major anthropogenic source of atmospheric carbon dioxide.

A portfolio of carbon sequestration technologies is being explored in order to address the substantial environmental concerns exponentially increasing atmospheric CO_2 levels present. No technology is currently poised to take a leading role. A combination of technologies is needed to address this long-term, complex problem.[1,2] Several "short-term" economically-viable technologies are being explored for their potential to be implemented relatively quickly. However, these options, such as improved energy generation efficiency, inexpensive renewable energy sources, forestation, switching from coal to oil/gas, etc., are limited in their mitigation capacity. As such, they are being explored to buy time until other middle to long term technologies can be developed.[1,2] Terrestrial sequestration (manipulating the terrestrial biosphere to enhance its ability to sequester carbon) in particular, offers good potential as a critical bridging technology until large capacity, long-term technologies can be developed.[2] However, any adjustments to the biosphere must be undertaken with the utmost caution, due to the wide ranging potential for ripple effects in the ecosystem.

Long-term options for reducing anthropogenic carbon dioxide emissions focus on the use of (i) renewable and carbon-free energy (e.g., biomass, nuclear, wind, and solar generated power), and (ii) fossil-fuel energy combined with CO_2 sequestration.[1,2] Serious concerns surround nuclear energy in the areas of waste disposal, safety and nuclear proliferation, leaving it unlikely to play a major role. Cost, intermittent supply, and geographic restrictions provide formidable challenges to the expanding the role of renewable energy generation. The fossil fuel industry already has a successful record of scaling up to meet world energy demands and is well equipped to continue to supply the world's energy needs for centuries to come *if (i) suitable, environmentally benign, long-term CO_2 storage/disposal technology can be developed and (ii) sequestration technology costs can be reduced to a competitive level*.[1-5]

Proposed long-term (high-capacity) sequestration technologies can be grouped in two categories (i) long-term storage (e.g., ocean, geological sequestration) and disposal (mineral sequestration).[1,2] Each option benefits from very large sequestration capacity. CO_2 stored in concentrated form has to be monitored and protected against sudden release, at considerable ongoing expense. Sudden emission must be avoided, as it can have lethal consequences, since CO_2 is a heavy-than-air asphyxiating gas.[7,8] Slow seepage from storage reservoirs must also be prevented, as inadequate containment will only postpone the adverse environmental consequences of increasing atmospheric CO_2 levels. Without adequate containment, long-term CO_2 storage of the magnitude proposed may create a global environmental debt that future generations may not be equipped to deal with.

Carbon dioxide mineral sequestration inherently avoids the problems associated with long-term storage by converting CO_2 into geologically stable mineral carbonates, such as ($CaCO_3$) or magnesite ($MgCO_3$). Only non-toxic, inert materials that already exist in vast quantities in nature (e.g., in Grand Canyon National Park, Arizona) are generated by mineral sequestration.[4,9] Thus, mineral sequestration can clearly provide environmentally benign carbon sequestration. The primary challenge for sequestration via mineral carbonation is cost-competitive process development.

Mg-rich silicate minerals, such as olivines and serpentines, offer excellent potential as mineral carbonation feedstock materials. First, silicate mineral carbonation is strongly exothermic (e.g., the overall energy released during forsterite (Mg_2SiO_4) and serpentine ($Mg_3Si_2O_5(OH)_4$) carbonation is 23 and 15 kcal/mol, respectively), providing clear energy and process cost advantages.[9-15] Second, Mg-rich silicates, especially serpentines, already exist in readily minable deposits in quantities far in excess of

that needed to carbonate all the CO_2 that could be emitted from the world's fossil fuel reserves.[4,11,14] Evaluation of Mg-rich silicate minerals and their derivatives as potential low-cost feedstock materials for mineral carbonation is a primary focus of the CO_2 Mineral Sequestration Working Group in its efforts to evaluate the economic viability of mineral carbonation as a long-term CO_2 sequestration technology. The Group, managed by DOE, consists of members from the Albany Research Center, Arizona State University, Los Alamos National Laboratory, National Energy Technology Laboratory, and Science Applications International Corporation.

The major hurdle to developing an economically viable process is achieving essentially complete carbonation, which naturally occurs over geological time, on an industrial time scale.[11] This is essential, as carbonation reaction rates are inversely related to process cost.[11] Carbonation reaction rates depend on a wide variety of process and materials parameters, offering good potential for rate enhancement. However, the effects that many of these parameters have on carbonation processes are not well understood, especially at the atomic level, severely limiting their effective use.

Mg-rich lamellar hydroxides (e.g., brucite and serpentine) are appealing as candidate mineral sequestration feedstock materials as (i) they are widely available at low cost (e.g., serpentines) and (ii) dehydroxylation can disrupt their structure down to the atomic level, with the potential to substantially enhance carbonation reactivity.[16] $Mg(OH)_2$ was chosen as a prototype material for initial study of the associated dehydroxylation-carbonation mechanisms due to (i) its chemical and structural simplicity,[16] (ii) interest in $Mg(OH)_2$ gas-solid carbonation as a CO_2 mineral sequestration process component,[10,12,17] and (iii) its chemical and structural similarity to other, more complex, Mg-rich lamellar hydroxide minerals (e.g., serpentine), whose carbonation reaction processes offer exciting low-cost potential.[18] The chemical and structural similarities between brucite and serpentine are shown in Figure 1. Their similarities also extend to their heats of carbonation (i.e., 19 kcal/mol vs. 15 kcal/mol for brucite and serpentine carbonation, respectively).[15] Developing a fundamental understanding of these mechanisms will establish the foundation necessary to enhance reaction rates and reduce process costs via materials and process engineering.

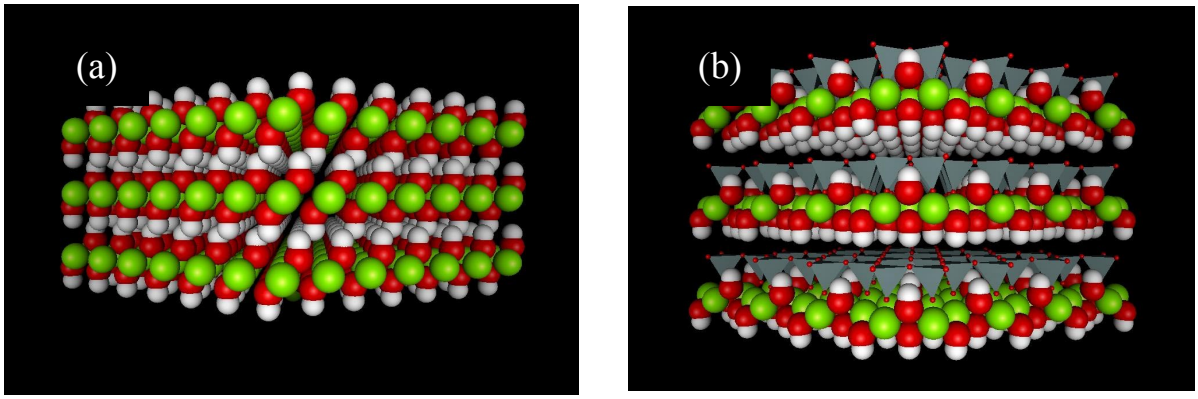

Figure 1. A lamellar view of the Mg-rich lamellar hydroxide minerals (a) brucite, $Mg(OH)_2$, and (b) serpentine (lizardite). Note the close structural similarities, with both structures containing Mg lamella and hydroxide lamella. The green, red and white spheres correspond to the Mg, O, and H atom positions, respectively. The grey tetrahedra with small red spheres at the corners correspond to the silica (SiO_4) groups connected in lamellar sheets, which also contain hydroxyl groups.

MATERIALS AND METHODS

Natural single crystal brucite from Delora, Canada was the primary starting material for dehydroxylation/rehydroxylation carbonation studies. Single crystal fragments from the host crystal were used to minimize any effect of structural defects initially in the samples and to facilitate optical microscopy observation of the material defects that inherently form during dehydroxylation/rehydroxylation carbonation processes. X-ray powder diffraction was used to structurally characterize the starting material [a=3.147(1) Å and c=4.765(1) Å], in good agreement with the known parameters for brucite [a=3.147 Å and c=4.769 Å].[19] Mass loss at 1500 ^{o}C was 99.7% of that expected for MgO formation. Elemental (proton-induced X-ray emission and total carbon) analysis found the material to contain 0.16% Mn, 0.06% C, 0.01% Cl and 0.01% Si by weight. Single crystal fragments typically weighing a few mg and a few mm in lateral extent were used for thermogravimetric analysis, optical microscopy, and elemental analysis studies. Smaller fragments from the same crystal were used in our recent atomic level investigation of the *in situ* $Mg(OH)_2$ dehydroxylation process.[20] Alfa Aesar $Mg(OH)_2$ powder (95-100.5%) was used as received for comparative TGA/elemental analysis studies, as indicated.

Thermogravimetric analysis (TGA) studies of *in situ* $Mg(OH)_2$ dehydroxylation/rehydroxylation carbonation processes were performed using a Setaram TG92 thermal analysis system. Sample weight changes were measured as a function of temperature and atmosphere for similarly sized $Mg(OH)_2$ single crystal fragments (three ~5 mg crystals/run) or $Mg(OH)_2$ powder contained in alumina crucibles. Absolute weight sensitivity was 1 μg. Weight changes were observed to better than ± 0.1%. The resulting TGA samples were evacuated and stored in a He-filled glovebox (Vacuum Atmospheres Corp.; ≤ 1 ppm total O_2 + H_2O) prior to elemental analysis to avoid atmospheric CO_2 or H_2O uptake. Total hydroxide, carbonate and oxide compositions were determined using a Perkin Elmer 2400 Series II CHNS Analyzer. Comparative standards gave total carbonate and hydroxide errors of ≤ 2 and 6 mol %, respectively. The total oxide present was determined by difference. Partially carbonated samples for optical microscopy observation were prepared using a high-pressure autoclave, vitreous silica sample containers, and dry CO_2 (99.99%). The optical microscope used was a Mititoyo Ultraplan FS-110 microscope with a magnification range of 200-1000X.

Ab initio density functional theory calculations and semi-empirical electron-gas modeling based on the VIB method [21] were used to follow the enthalpies and free energies of formation of the intermediate lamellar oxyhydroxides as a function of temperature and composition. Compositional behavior was investigated using periodic lamellar phases to represent discrete compositions in the oxyhydroxide solid solution series. These studies follow earlier work on simple hydroxides based on the closely related PIB method.[22] Bulk periodic ordered phases of stoichiometry $Mg_{x+y}O_x(OH)_{2y}$ (following a brucite-like motif with space group symmetry $P\bar{3}m1$) were structurally optimized, as previously.[20,23] *Ab initio* density functional theory calculations based on GGA[24,25] were carried out for bulk MgO, $Mg(OH)_2$, $Mg_{x+y}O_x(OH)_{2y}$ and molecular H_2O. These calculations yield structural parameters typically within a percent of the corresponding experimental values. Our GGA estimate of the enthalpy of formation for $Mg(OH)_2$ from MgO and H_2O (g), 17.9 *kcal/mol*,[26,27] compares very well with the observed value of 19.4 *kcal/mol*,[28] while a relative energy for the 50% dehydroxylation intermediate ½{E[$Mg_2O(OH)_2$] – E[MgO] – E[$Mg(OH)_2$]} of 2.8 kcal/mol is obtained. This is to be compared with the VIB estimate of 2.6 kcal/mol. The *ab initio* calculations were also used to derive a hydroxyl binding potential, required in the ionic models to stabilize the (OH) bond. We refer to this method as the semi-empirical VIB scheme, or SEVIB. In previous work[22] this bond was explicitly constrained, thereby precluding a quantitative treatment of dynamical and elastic behavior.

DEHYDROXYLATION/REHYDROXYLATION PROCESSES: FORMING CARBONATION REACTION INTERMEDIATES

As $Mg(OH)_2$ dehydroxylation is the first step in gas-phase carbonation, developing an atomic-level understanding of the associated reaction mechanisms is essential for understanding and optimizing the carbonation process. Furthermore, any intermediate materials that form during dehydroxylation can provide new carbonation reaction pathways, which may enhance carbonation reactivity.

During dehydroxylation, the $Mg(OH)_2$ crystal structure contracts by 50% perpendicular to and 5% parallel to its lamella, respectively.[29,30] $Mg(OH)_2$ and the product MgO maintain a unique crystallographic relationship during the process, as shown in Figure 2.

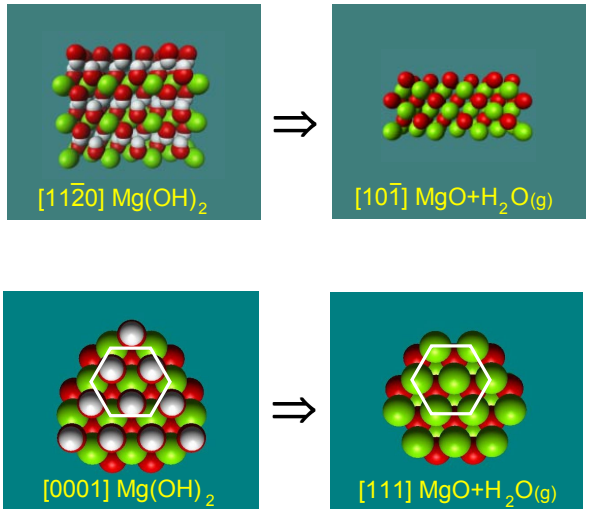

Figure 2. A lamellar view of the crystallographic relationship between $Mg(OH)_2$ and MgO during dehydroxylation, parallel (above) and perpendicular (below) to the $Mg(OH)_2$ lamella. The green, red and white spheres correspond to the Mg, O, and H atom positions, respectively.

As a result, the lattice experiences high levels of elastic stress during dehydroxylation, which can generally disrupt the structure down to the atomic level. The associated stress also has the intriguing ability to facilitate lattice surface reconstruction to form novel MgO nanostructures during low-temperature calcination.[29-34] These structures can have quite high surface areas (e.g., 100-200 m^2/g), which may be able to facilitate mineral carbonation under suitable reaction conditions.

$Mg(OH)_2$ dehydroxylation has long been viewed as a simple two-phase process: $Mg(OH)_2 \rightarrow MgO + H_2O$.[29-34] However, our recent atomic-level observations of the dehydroxylation process have found the process can offer a rich range of intermediate materials, with the potential to act as bridges to new carbonation reaction pathways.[20,23] *In situ* environmental-cell (E-cell) dynamic high-resolution transmission electron microscopy (DHRTEM) imaging and selected area diffraction (SAD) observations were combined with advanced computational modeling to discover $Mg(OH)_2$ dehydroxylation proceeds via lamellar nucleation and growth. Initially, neighboring hydroxide groups combine to form water and oxide locally, with the water escaping from the lamella as it collapses, as shown in reaction 1.

$$(1) \qquad \cdots OH/Mg/OH/OH/Mg/OH\cdots \rightarrow \cdots OH/Mg/O/Mg/OH\cdots + H_2O$$

Additional oxide layers nucleate and grow nearby to form lamellar oxyhydroxide regions within the brucite matrix. The resulting oxide lamella are randomly distributed within the oxyhydroxide regions, creating a low-dimensional solid solution of oxide and hydroxide lamella. As dehydroxylation continues, these regions continue to nucleate and grow parallel and perpendicular to the lamella until the host brucite matrix is consumed.[20,23]

The solid solution nature of the oxyhydroxide regions indicates they must accommodate the lamellar stress associated with the different in-plane packing distances of ideal $Mg(OH)_2$ and MgO layers, 3.15Å and 2.98Å, respectively. Our recent SEVIB modeling investigations of in-plane packing distance vs. oxide composition confirm the lamellar solid solution character of the oxyhydroxides.[20,23] Overall, these regions follow a lamellar form of Vegard's Law,[35] where, to a first approximation, the in-plane packing distance is a weighted average of the ideal distances for the oxide and hydroxide layers present locally. Thus, *in situ* observation of the in-plane packing distance during dehydroxylation allows direct evaluation of the composition of the lamellar oxyhydroxide regions. Table 1 compares the range of oxyhydroxide compositions [$Mg_{x+y}O_x(OH)_{2y}$] previously observed based on the range of in-plane packing distances measured by SAD during dehydroxylation.[20,23,29,30] Our recent SAD studies of the *in situ* dehydroxylation process[20] are presented together with a reassessment of previous low-magnification TEM and SAD observations.[29,30]

Table 1: Intralamellar In-Plane Packing Distances Observed by SAD for the Oxyhydroxide, $Mg_{x+y}O_x(OH)_{2y}$, Regions and the $Mg(OH)_2$ Host Matrix during *In Situ* Dehydroxylation. The Composition Range of the Oxyhydroxide Regions is Based on VIB-based Non-Empirical Electron Gas Modeling.

Study	$Mg(OH)_2$ Matrix (packing distance)	$Mg_{x+y}O_x(OH)_{2y}$ (packing distance)	$Mg_{x+y}O_x(OH)_{2y}$ composition (% $Mg(OH)_2$)
Gordon & Kingery[29]	3.15Å	3.14 → 2.98 Å	94% → 0%
Kim, et al.[30]	3.15Å	3.00 → 2.98 Å	12% → 0%
McKelvy, et al.[20]	3.15Å	3.04 → 2.98 Å	35% → 0%

The in-plane packing distance and composition of the $Mg(OH)_2$ matrix remains unchanged during dehydroxylation and is largely unaffected by the nucleation and growth of the oxyhydroxide regions. However, essentially the full solid-solution range of in-plane packing distances and lamellar hydroxide/oxide compositions are observed for the oxyhydroxide regions. This indicates a broad new range of dehydroxylation intermediates are accessible, opening the door to a range of potential new carbonation reaction pathways. These observations are consistent with SEVIB calculations of the relative free energies of formation, ΔG, for the oxyhydroxides shown in Table 2.* ΔG for the oxyhydroxides is quite low ($\leq$ 2.3 kcal/mol) over a broad temperature range and throughout the solid solution series. This allows the lamellar hydroxide structure to guide the reaction process at the atomic level, resulting in metastable oxyhydroxide intermediate formation. The range of oxyhydroxide compositions observed under different dehydroxylation conditions in Table 1 is indicative of competition between relatively fast-nucleation/slow-growth[30]

* The free energies, ΔG, for the intermediate oxyhydroxides are calculated relative to that expected for hypothetical MgO + $Mg(OH)_2$ mixed phase regions.

Table 2: Oxyhydroxide Free Energies Relative to Stoichiometrically Equivalent Amounts of $Mg(OH)_2$ and MgO (ΔG in kcal/mol) as a Function of Temperature.

	Composition (% Hydroxide Lamella in $Mg_{x+y}O_x(OH)_{2y}$)				
Temperature	0% [MgO]	33.3%	50%	66.7%	100% [$Mg(OH)_2$]
127 °C	0.00	+1.20	+2.29	+1.59	0.00
177 °C	0.00	+1.01	+2.08	+1.40	0.00
327 °C	0.00	+0.82	+1.87	+1.21	0.00
477 °C	0.00	+0.63	+1.67	+1.02	0.00
627 °C	0.00	+0.44	+1.46	+0.83	0.00

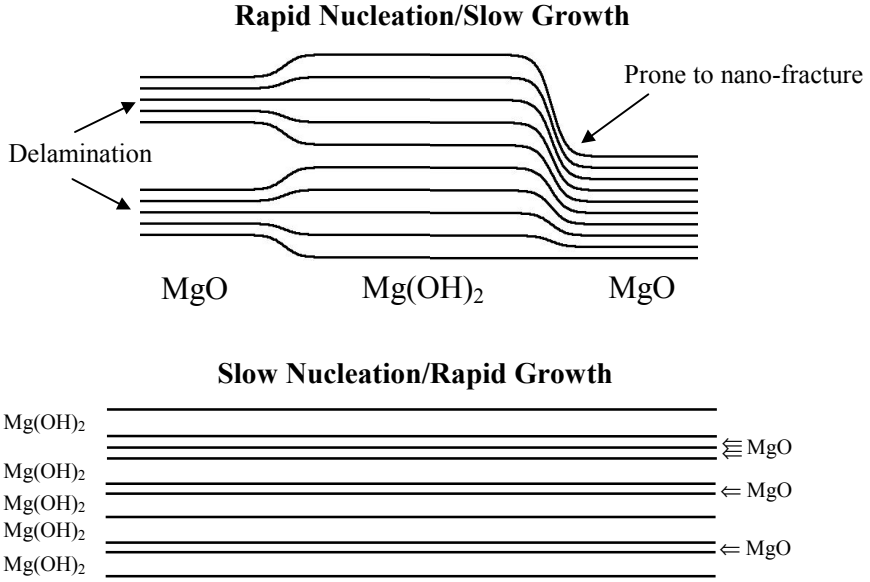

Figure 3. Models of relatively rapid nucleation/slow growth and slow nucleation/rapid growth lamellar nucleation and growth processes. The two-phase ($Mg(OH)_2$ + MgO) and homogeneous lamellar oxyhydroxide character of these processes is consistent with previous low-magnification TEM SAD observations of $Mg(OH)_2$ dehydroxylation (Table 1).

(primarily two-phase) and slow-nucleation/fast-growth[29] (primarily lamellar oxyhydroxide intergrowth) lamellar processes, as shown in Figure 3. Higher and lower temperatures are generally expected to favor nucleation and growth, respectively, offering additional possibilities for dehydroxylation process control.[36]

Competition between lamellar nucleation and growth will directly impact high-surface-area MgO nanostructure formation as well. As shown in Figure 3, layer bending during dehydroxylation can lead to delamination of the layers and nanofracture perpendicular to the layers. Delamination and cracking are a well-known component of the dehydroxylation process[29] and extend to dehydroxylation-carbonation processes as well, as shown in Figure 4.[12] Since, the elastic stress present locally depends on the

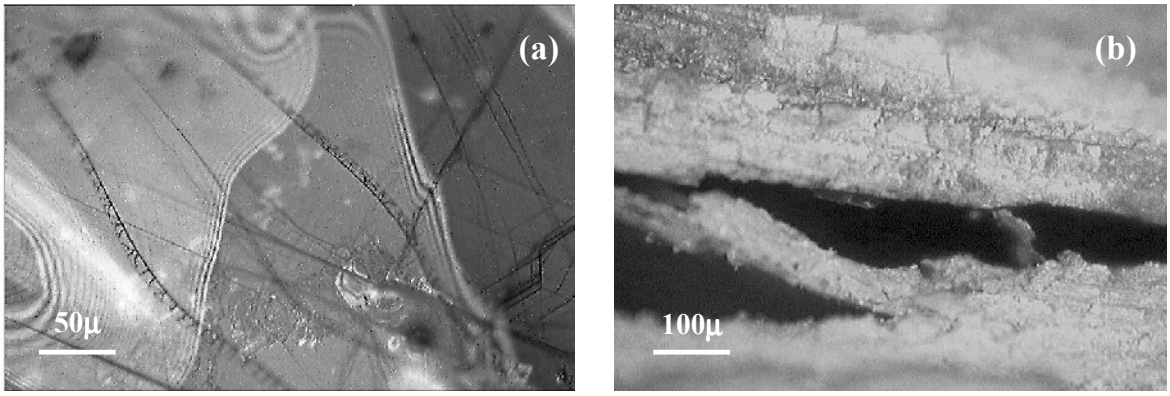

Figure 4. Bright-field optical micrographs of partially dehydroxylated and carbonated $Mg(OH)_2$ early during the reaction process.[23] (**a**) cracking and lamellar strain fields viewed perpendicular to the $Mg(OH)_2$ lamella. (**b**) delamination and cracking viewed parallel to the lamella.

competition between nucleation and growth, so will the nature of the nanofragments that form. Once these high-surface-area fragments form, they can surface reconstruct to more stable forms, such as the cubic MgO nanostructures that form during low-temperature (e.g., 300-500 ^{o}C) $Mg(OH)_2$ dehydroxylation.[29,30,32,33] Overall, delamination and cracking during dehydroxylation can disrupt macroscopic crystals into micron to submicron particles that are comprised of intergrown MgO nanostructures. Combining the formation of these structures with the discovery of lamellar oxyhydroxide intermediate formation offers broad new potential to enhance carbonation reactivity. Furthermore, low-temperature dehydroxylated MgO containing low residual hydroxide concentrations (e.g., 5-10%) can fully rehydroxylate via exposure to H_2O (g) at ambient temperature.[34] This extends the range of potential carbonation reaction pathways to include rehydroxylation, as well as dehydroxylation processes.

ENHANCING CARBONATION REACTIVITY VIA DEHYDROXYLATION/REHYDROXYLATION INTERMEDIATE FORMATION

Recently, we discovered rehydroxylation processes can dramatically enhance gas-phase carbonation reactivity, underscoring the potential of oxyhydroxide intermediate materials to enhance carbonation reactivity.[23] *In situ* thermogravimetric analysis (TGA) studies were combined with *ex situ* carbon and hydrogen elemental analysis, as shown in Figure 5 and Table 3. Single crystal fragments were initially 93% dehydroxylated at 375 ^{o}C under dry helium to form high surface area intermediates for carbonation reactivity studies. Subsequent exposure to dry or humid CO_2 at 375 ^{o}C resulted rapid carbonation of ~ 1% of the sample, after which carbonation ceased. This indicates only a very small percentage of the material possessed reactive carbonation intermediate sites at 375 ^{o}C. Cooling to 23 ^{o}C resulted in little change for dry CO_2. However, cooling to 23 ^{o}C under humid CO_2 induced rapid rehydroxylation and carbonation, indicating the formation of transitory oxyhydroxide intermediate materials can dramatically enhance carbonation reactivity. The potential of these intermediates to enhance carbonation reactivity is underscored by the over 350 ^{o}C ***decrease*** in reaction temperature that accompanied the dramatic increase in carbonation reactivity.

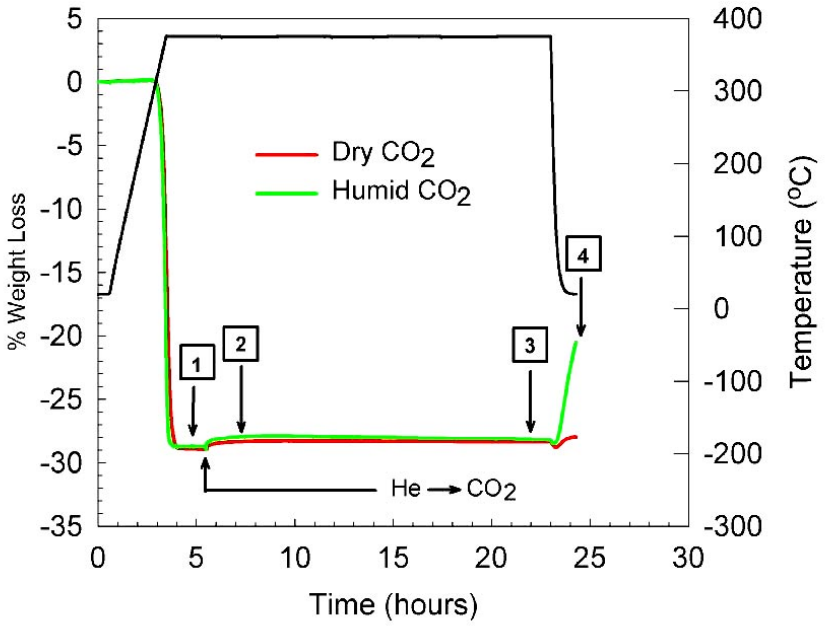

Figure 5. *In situ* thermogravimetric analysis studies of carbonation of low-temperature (375 °C) calcined $Mg(OH)_2$.[23] After stabilizing at ~ 93% dehydroxylation (position 1), the atmosphere was changed from dry He to humid (~ 70% humidity) and dry CO_2 for the separate runs at 375 °C, as shown. Slight carbonation (~ 1%) occurs initially (by position 2), but does not continue (position 3). Cooling to ambient temperature (position 4) results in little reaction under dry CO_2, whereas humid CO_2 shows strong carbonation and rehydroxylation behavior, as confirmed by carbon and hydrogen elemental analysis. The slight dip between position 3 and 4 is associated with instrumental/buoyancy effects.

Table 3: Sample Compositions* for Reaction Positions in Figure 5[23]

Reaction	Humid CO_2			Dry CO_2		
Position	%$MgCO_3$	%MgO	%$Mg(OH)_2$	%$MgCO_3$	%MgO	%$Mg(OH)_2$
1	0.0	93.0	7.0	0.0	93.6	6.4
2	1.1	91.9	7.0	0.9	92.7	6.4
3	1.1	92.5	6.4	0.9	92.9	6.2
4**	8.1	76.6	15.3	1.4	92.4	6.2

* Compositions are given in mol % and determined by weight change for positions 1-3, as described in the text.

** The final compositions for humid and dry CO_2 are determined by total C & H analysis and TGA assuming only carbonation occurs, respectively. The humid compositions agree well with the final weight gain observed on cooling (between position 3 and 4; 7.8% TGA vs. 8.0% estimated from C & H elemental analysis). The dry compositions agree well with those from C & H analysis (1.2% $MgCO_3$, 95.3% MgO, 3.5% $Mg(OH)_2$). For the dry CO_2 run, the slight increase in %$MgCO_3$ /%$Mg(OH)_2$ may be associated with traces of H_2O left in the TGA system from dehydroxylation.

Figure 6 shows thermogravimetric analysis of a similar dehydroxylation/carbonation process using reagent grade Alfa Aesar $Mg(OH)_2$. The powder is initially 92% dehydroxylated under dry helium by heating at 2°C/min to 375 °C and holding at 375 °C for 2.75 hours. Then the temperature is cooled to 23 °C at 20 °C/min., with the reaction gas simultaneously changed to humid (~70%) CO_2. Rehydroxylation/carbonation started well before sample cooling was complete (~ 200 °C), with a slight acceleration in weight gain at ~ 110 °C, which likely coincides with the onset of rehydroxylation. After a little over an hour, the reaction rate begins to slow significantly. Similar studies showed this slowing is a

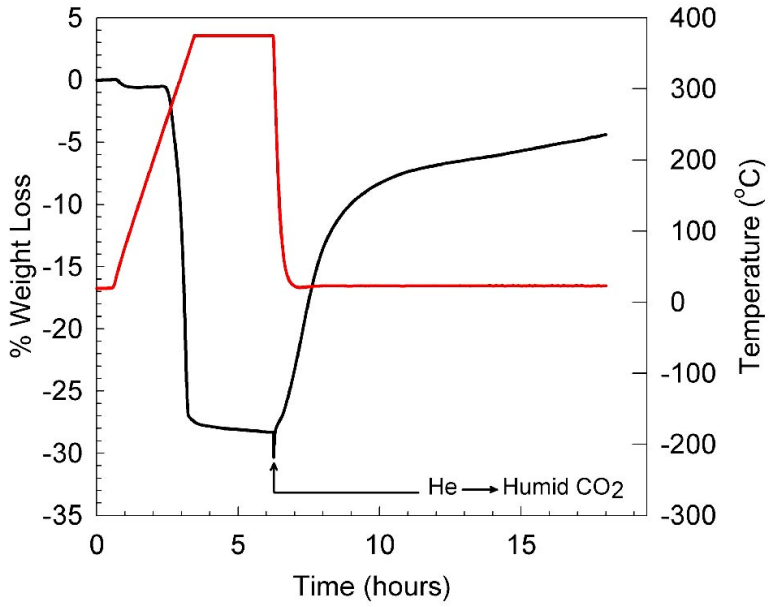

Figure 6. *In situ* thermogravimetric analysis of carbonation of low-temperature (375 °C) calcined $Mg(OH)_2$. After achieving 92% dehydroxylation at 375 °C under dry helium, the atmosphere was changed to humid (~ 70% humidity) CO_2, while simultaneously initiating cooling at 20 °C/min to 23 °C. The slight dip on switching from He to humid CO_2 is an artifact of the gas changeover process. The strong weight gain after the changeover is associated with rehydroxylation/carbonation.

function of sample size, with smaller samples rehydroxylating and carbonating more rapidly. This suggests the sample is reducing the partial pressure of water vapor locally in the TGA crucible, slowing both rehydroxylation and carbonation. Flow through studies are currently underway that supply CO_2 with constant humidity throughout carbonation to further explore this process. Upon completion of the reaction, elemental analysis gave a sample composition of 18.1 mol % $MgCO_3$, 37.0 mol % $Mg(OH)_2$, and 44.9 mol % MgO, in good agreement with the total mass change. X-ray powder diffraction showed no clear peaks indicative of crystalline carbonate formation, indicating the carbonate formed is poorly ordered (e.g., amorphous), as one might expect for a low temperature reaction process. Recently, we have also observed similar carbonate formation during *in situ* parallel electron energy loss spectroscopy investigation of the rehydroxylation-carbonation process (via E-cell DHRTEM). These studies will be the subject of a future publication.

CONCLUSIONS

Transitory intermediate materials that form during $Mg(OH)_2$ dehydroxylation/rehydroxylation, such as the lamellar oxyhydroxide solid solution series, $Mg_{x+y}O_x(OH)_{2y}$, can substantially enhance carbonation reactivity. This is underscored by the observation of dramatically enhanced gas-phase carbonation reactivity *at ambient CO_2 pressure and temperature* during dehydroxylation. The lamellar oxyhydroxides have slightly positive free energies of formation (≤ 2.3 kcal/mol) relative to comparable amounts of $Mg(OH)_2$ and MgO over the reaction temperature range of interest, allowing the lamellar $Mg(OH)_2$ structure to guide the dehydroxylation process. The range of potential carbonation reaction pathways available via dehydroxylation/rehydroxylation intermediate formation is illustrated in Figure 7. Although the concentration of carbonation reactive intermediates may be low at any given intermediate hydroxide composition, simultaneous dehydroxylation/rehydroxylation processes can provide continuous access to fresh, carbonation-reactive, intermediate materials that can greatly enhance overall carbonation reactivity. Integrating enhanced intermediate reactivity with the ability to form high-surface-area nanostructured materials during dehydroxylation further extends this potential. The dehydroxylation/rehydroxylation/carbonation processes observed for $Mg(OH)_2$ are directly associated with its prototypical lamellar mineral character. This suggests similar mechanisms may be generally applicable to other Ca and/or Mg-rich lamellar hydroxide based materials. The serpentine-based minerals (e.g., lizardite, antigorite and chrysotile) are of particular interest in this regard, due to their wide availability as low-cost mineral carbonation feedstock materials.[9-15,18] Control of lamellar hydroxide mineral dehydroxylation/rehydroxylation processes offers excellent potential to enhance mineral carbonation reaction rates and significantly reduce CO_2 mineral sequestration process costs.

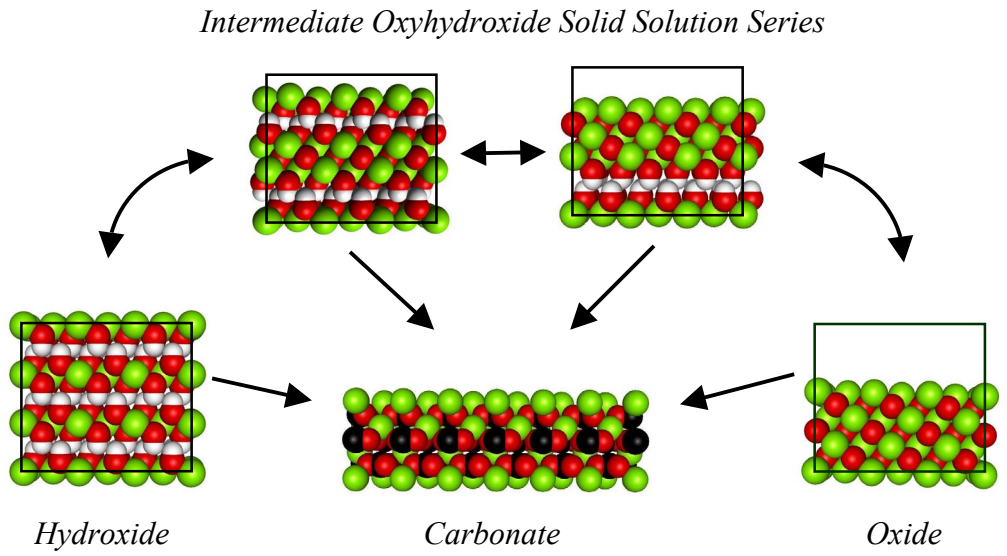

Figure 7. Possible $Mg(OH)_2$ carbonation reaction pathways during dehydroxylation and/or rehydroxylation. The intermediate lamellar oxyhydroxide solid solution series, $Mg_{x+y}O_x(OH)_{2y}$, is represented by nominal compositions of $Mg_3O(OH)_4$ and $Mg_3O_2(OH)_2$. The green, red, white, and black spheres correspond to the Mg, O, H, and C atom positions, respectively. Whereas MgO and $Mg(OH)_2$ can form by dehydroxylation and rehydroxylation, respectively (potentially cycling back and forth at low temperatures), carbonate formation is thermodynamically dictated as a one way reaction (below the $MgCO_3$ decomposition temperature).

ACKNOWLEDGMENTS

We gratefully acknowledge the National Energy Technology Laboratory of the U.S. Department of Energy for support through grants DE-FG26-98FT40112 and DE-FG26-99FT40580. We also thank the Center for Solid State Science for use of the Goldwater Materials Science Laboratories, including the Materials Facility, the Goldwater Materials Visualization Facility, the Optical Microscopy Laboratory and the Ion Beam Analysis Facility.

REFERENCES

1. Herzog, H.; Drake, E.; Adams, E. *CO_2 Capture, Reuse, and Storage Technologies for Mitigating Global Climate Change*, DOE Report No. DE-AF22-96PC01257 (1997).
2. Carbon Sequestration Research and Development, Offices of Science and Fossil Energy, U.S. Department of Energy (December 1999).
3. Current estimates of world coal reserves are 10,000 billion tons. Less than 0.1% is currently consumed annually (see ref. 4,5).
4. United Nations, *1991 Energy Statistics Yearbook*, New York, 1993.
5. Climate Change 1995: The Science of Climate Change. Contribution of Working Group I to the Second Assessment Report of the Intergovernmental Panel on Climate Change, Cambridge University Press, 1995.
6. Kyoto Protocol to the U.N. Framework Convention on Climate Change, December 1997.
7. Cling, G.; Clark, M.; Compton, H.; Devine, J.; Evans, W.; Humphrey, A.; Koenigsberg, E.; Lockwood, J.; Tuttle, M.; Wagner, G. *Science* **286**, 169 (1986).
8. Freeth, S. *Geochemical Journal* **28**, 163 (1994).
9. Lackner, K.; Wendt, C.; Butt, D.; Joyce Jr., E.; Sharp, D. *Energy* **20**, 1153 (1995).
10. Butt, D.P.; Lackner, K.S.; Wendt, C.H.; Benjamin, A.S.; Currier, R; Harradine, D.M.; Holesinger, T.G.; Park, Y.S.; Rising, M. *World Resource Review*, **9 (3)**, 324 (1997).
11. Lackner, K.; Butt, D.; Wendt, C.; Goff, F.; Guthrie, G. Los Alamos National Laboratory Technical Report LA-UR-97-2094 (1997).
12. Butt, D.; Lackner, K.; Wendt, C.; Conzone, S.; Kung, H.; Lu, Y.; Bremser, J. *J. Am. Ceram. Soc.* **79**, 1892 (1996).
13. Lackner K.; Butt, D.; Wendt, C. *Energy Convers. Mgmt*. **38**, S259 (1997).
14. Lackner K.; Butt, D.; Wendt, C.; Sharp, D. *Proc. 21st Int. Conf. Coal Util. Fuel Syst.*; Sakkestad, B.: Ed. Coal and Slurry Tech. Assoc., Washington, D.C., pp. 133-144 (1996).
15. Lackner K.; Butt, D.; Wendt, C. *Proc. 22nd Int. Conf. Coal Util. Fuel Syst.*, pp. 419-430 (1997); also Los Alamos National Laboratory Technical Report LA-UR-97-660.
16. Klein, C.; Hurlbert, C.S. *Manual of Mineralogy*, 21st edn (Wiley, New York, 1993).
17. Wendt, C.H.; Butt, D.P.; Lackner, K.S.; Ziock, H.J. Los Alamos National Laboratory, Technical Report: LA-UR-98-4529 (1998).
18. O'Connor, W.K.; Dahlin, D.C.; Nilsen, D.N.; Walters, R.P.; Turner, P.C.; *Proc.25th Int. Conf. Coal Util. Fuel Syst.*, pp 153-164 (2000).
19. U.S. Nat. Bur. Stand. Circ. **539**, 6 30 (1956).
20. McKelvy, Michael J.; Sharma, R.; Chizmeshya, Andrew V.G.; Carpenter, Ray W.; Streib, Ken (submitted).
21. Chizmeshya, A.; Zimmermann, F.M.; LaViolette, R.A.; Wolf, G.H. *Phys. Rev. B,* **50**, 15559, (1994).
22. LeSar, R.; Gordon, R.G. *Phys. Rev. B,* **25**, 7221 (1982).
23. McKelvy, Michael J.; Sharma, Renu; Chizmeshya, Andrew V.G.; Bearat, Hamdallah; Carpenter, R.W.; *Proc. 25th Int. Conf. Coal Util. Fuel Syst.*, pp. 897-908 (2000).
24. We employ the PWGGA functional as implemented within the CRYSTAL98 periodic DFT and Hartree-Fock program. Saunders, V.A., et al. *CRYSTAL98 User's Manual*, University of Torino, 1998.
25. We carried out a full suite of GGA calculations of the compression equation of state of MgO, $Mg(OH)_2$ and several oxyhydroxide intermediates. Equilibrium lattice constants and internal structural parameters reproduced experimental values to within 1%.

26. We follow Refson *et al.* [Ref. 27] in adding the sublimation energy of ice to our molecular H_2O energy to obtain the formation energy at 0 K.
27. Refson, K.; Wogelius, R.A.; Fraser, D.G.; Payne, M.C.; Lee, M.H.; Milman, V. *Phys. Rev. B,* 52, 10823 (1995).
28. James, A.M.; Lord, M.P. *Macmillan's Chemical & Physical Data*, (Macmillan Press LTD, London, 1992).
29. Gordon, R.; Kingery, W. *J. Am. Ceram. Soc.* **49**, 654 (1966) and **50**, 8 (1967).
30. Kim, M.G.; Dahmen, U.; Searcy, A.W. *J. Am. Ceram. Soc.* **70**, 146 (1987).
31. Green, J. *J. Mater. Sci*. **18**, 637 (1983).
32. Moodie, A.F.; Warble, C.E. *J. Cryst. Growth* **74**, 89 (1986).
33. Thangaraj, N.; Westmacott, K.H.; Dahmen, U. *Ultramicroscopy* **37**, 362 (1991).
34. Ribeiro Carrott, M.M.L.; Carrott, P.J.M. *Characterization of Porous Solids III*, Studies in Surface Science and Catalysis, **87**, 497 (1994).
35. Wells, A.F. *Structural Inorganic Chemistry* 5th edn (Clarendon Press, Oxford, 1984), pg 1294.
36. The reaction temperatures for the various *in situ* SAD studies are likely significantly different, due to the variation in electron beam heating expected for different *in situ* reaction conditions. Based on *ab initio* density functional theory calculations and non-empirical electron-gas modeling, the combined thermodynamic and kinetic stability of the intermediate oxyhydroxides is expected to generally increase for higher oxide layer concentrations, slowing the dehydroxylation process [Ref. 20].